XLI CILAMCE
XLI Ibero-Latin American Congress on Computational Methods in Engineering
16-19 November, 2020 FOZ DO IGUAÇU PARANÁ - BRAZIL

Experimental validation and numerical simulation of a direct-expansion solar-assisted heat pump for heating water

André G. de Oliveira[1], Hélio A. G. Diniz[2], Willian M. Duarte[3], Luiz Machado[4], Raphael N. Oliveira [5]

[1]*Programa de Pós Graduação em Engenharia Mecânica Universidade Federal de Minas Gerais (UFMG*
Av. Antonio Carlos, 6627,Belo Horizonte - MG, 31270-901, Brazil
andreqix@hotmail.com[1], helioufmg@gmail.com[2], willianmoreiraduarte@gmail.com[3], luizm@demec.ufmg.br[4],
rphnunes@demec.ufmg.br[5]

Abstract. In this work, a simulation model was developed to predict the thermal performance and discharge temperature of a heat pump and compare with the experimental data. In this analysis a lumped model will be used for each component of the system. The effect of various parameters, including collector area, storage volume, solar radiation, windy speed, and atmospheric pressure was considered in the simulation. In this case will be carried out considering the climatic conditions in the city of Belo Horizonte. This model was experimentally validated using a direct expansion heat pump assisted by solar energy (DX-SAHP) equipped with a thermostatic expansion valve. The performance of the heat pump simulation was compared with experimental results. The mean absolute deviation mean deviation between the experimental COP and theoretical COP was 4.2±4.8% and 2.9±5.2%, respectively. The mean absolute deviation mean deviation between the experimental and theoretical compressor outlet temperature was 3.3±2.0% and -2.0±2.0%, respectively.

Keywords: Solar-assisted heat pump, Model uncertainty, Discharge temperature, COP.

1 Introduction

One way to reduce electricity consumption is to use direct-expansion solar-assisted heat pump (DX-SAHP) instead of electric heaters. Domestic hot water, after air conditioning, has become the second largest contributor to residential building energy consumption, as the cost of energy continues to rise, it becomes important to save energy. DX-SAHP use the same mechanical principles as refrigerators and air conditioners but the collector and evaporator functions are combined into one unit, where the refrigerant from the condenser gets evaporated by incident solar energy. What makes the heat pump more advantageous is its high thermal efficiency, as investigated by Chua et al. [1].

The demand of heat pumps has been increased significantly due to higher efficiency of heating system grounded on the vapor compressor principle. In the literature consulted there are some models experimentally validated for DX-SAHP [2–8], but only in the work presented in [4] the authors compared the theoretical and experimental compressor outlet temperature. Predict the discharge temperature of the compressor is extremely important to increase the life of the compressor. High temperatures in the suction also increase the discharge temperature, resulting in the loss of viscosity of the lubricating oil and consequently breaking the compressor. Additionally, none of the models listed [2–8] obtained the uncertainty of variables calculated by the model. This work presents a mathematical model for a DX-SAHP that is validated experimentally comparing the results of COP and discharge temperature and the uncertainty of theoretical and experimental results are considered.

2 Mathematical Model

The refrigerant chosen for this work is the R134a. R134a is more suitable for DX-SAHP than R410A, R407C and R404A Chata et al. [9], it is the refrigerant most used in the recent studies of DX-SAHP [10–14] and, finally, it is the refrigerant used in the experimental tests used in the validation of the mathematical model [15].

To evaluate the performance of DX-SAHP for producing DHW (domestic hot water) a quasi-steady-state model was developed using Equation Engineering Solver (EES). The losses in the tubes between components was

considered negligible and for the inventory charge of the refrigerant, the pipeline was considered two meters long. The evaporator/solar collector and condenser was assumed as isobaric and a lumped model was used. Following is described the modeling equation for each component.

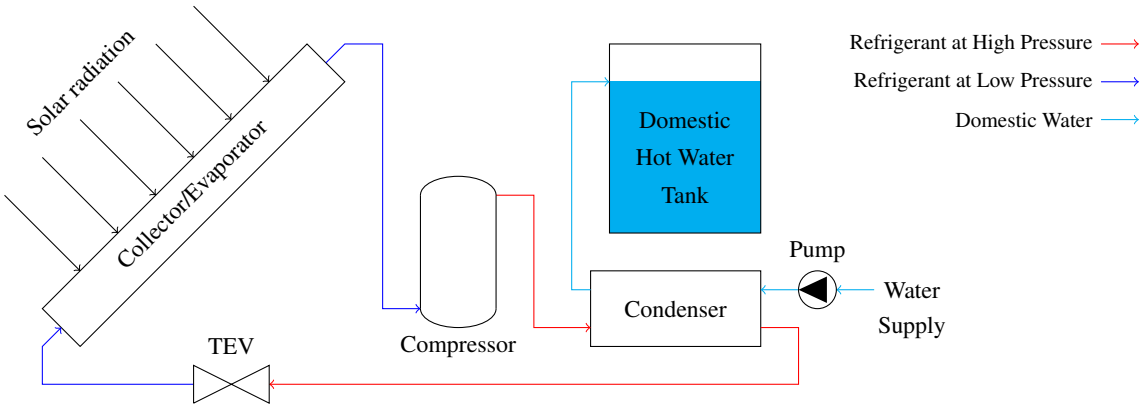

Figure 1. Schematic diagram of DX-SAHP used for a validation model.

2.1 Direct expansion solar evaporator

The heat transfer rate received by the refrigerant in the evaporator ($\dot{Q}_{re}$) is given by:

$$\dot{Q}_{re} = \dot{m}(i_1 - i_4) \tag{1}$$

where the subscript 4 refers to thermostatic valve outlet or evaporator inlet. To evaluate the energy gain in a flat plate collector ($\dot{Q}_{col}$) in steady-state condition [5] suggest the following equation:

$$\dot{Q}_{col} = A_e F'[S - U_L(\overline{T}_r - T_a)] \tag{2}$$

where A_e is the area of evaporator of the solar collector (1.65m^2), F' is the collector efficiency factor, S is the net radiation absolved per unit of area, U_L is overall heat loss coefficient, $\overline{T}_r$ is the average temperature of the refrigerant fluid and T_a is the ambient air temperature. The collector effectiveness factor is calculated using the Hottel-Whilliar-Bliss model described by [16], considering that the resistance to heat flow due the bond between the collector plate and tube can be neglected, is given by:

$$F' = \frac{1}{U_{ev}}\left\{W\left[\frac{1}{U_{ev}[D_o + F(W - D_o)]} + \frac{1}{\pi D_i h_i}\right]\right\}^{-1} \tag{3}$$

where the distance between the tubes in the evaporator is W, the fin efficiency is F, the outer diameter (8.73mm) is D_o, the inner diameter (9.53mm) is D_i, the internal convective coefficient is h_i that is calculated by the correlation proposed by Shah [17] for two phase flow and by the correlation proposed by Gnielinski [18] for single phase flow.

The fin efficiency can be evaluated by:

$$F = \frac{\tanh\left[(w - D_o)/2\sqrt{U_L/(k\delta)}\right]}{(w - D_o)/2\sqrt{U_L/(k\delta)}} \tag{4}$$

where δ is the fin thickness (1mm) and k is the thermal conductivity. The net radiation absolved is evaluated as made by Kong et al. [19]:

$$S = aI - \varepsilon\sigma(T_r^4 - T_s^4) \tag{5}$$

where the absorptivity is a, the solar radiation intensity normal to evaporator is I, the emissivity is ε, σ is the Stefane-Boltzmann constant and T_s is the sky temperature. The sky temperature was estimated by the method proposed by Gliah et al. [20] using the correlation of Angstrom presented by Berdahl and Fromberg [21] for sky emissivity (Eq. 6).

$$\varepsilon_{sky} = 0.734 + 0.0061T_{dp} \tag{6}$$

The overall heat loss coefficient proposed by Kong et al. [5] is determined by:

$$U_L = h_o + 4\varepsilon\sigma T_a^3 \tag{7}$$

where the external convective coefficient (h_o) is calculated by the collection of correlations for free and forced convection, depending on wind speed (u_w), for tilted flat plate listed by Neils and Klein [22].

2.2 Compressor model

The refrigerant mass flow rate ($\dot{m}$) in a constant rotation speed reciprocating compressor is given by Mohanraj et al. [12]:

$$\dot{m} = \rho_1 n V_s \eta_v \tag{8}$$

where ρ is the refrigerant density, n is the rotation speed (3500 rpm), V_s is the compressor swept volume (7.95 cm^3/rev.), η_v is the volumetric efficiency and the subscript 1 refers to compressor inlet or evaporator outlet. The compressor electric power consumption ($\dot{W}$), considering a isentropic compression process, is evaluated as follow Minetto [23]:

$$\dot{W} = \frac{\dot{m}(i_{2S} - i_1)}{\eta_g} \tag{9}$$

where η_g is the global efficiency and i is the refrigerant specific enthalpy and the subscript $2S$ refers to compressor outlet considering an isentropic process. The global and volumetric efficiency was determinate fitting equations proposed by Minetto [23] to the compressor performance map available in Embraco website. The global and volumetric efficiency is given by:

$$\eta_v = -0.0143 \left(\frac{P_2}{P_1}\right) + 0.915 \tag{10}$$

$$\eta_g = -0.0004 \left(\frac{P_2}{P_1}\right)^2 + 0.0104 \left(\frac{P_2}{P_1}\right) + 0.4839 \tag{11}$$

where P is the refrigerant pressure. The coefficient of determination (R^2) for volumetric efficiency is 97.6% and for global efficiency is 94.4%. In order to obtain with good precision, the discharge temperature of the compressor (T_2) an isentropic efficiency (η_i) of 85% was considered, and the entalphy at exit of the compressor evaluated as follow:

$$i_2 = \frac{i_{2S} - i_1}{\eta_i} + i_1 \tag{12}$$

2.3 Coaxial Condenser

The balance of energy in the refrigerant at the condenser is evaluated as follow:

$$Q_{cond} = \dot{m}_r (i_2 - i_3) \tag{13}$$

Assuming no heat loss in the coaxial condenser, the balance of energy in the water is given by:

$$Q_{cond} = \dot{m}_w C_w (T_{wo} - T_{wi}) \tag{14}$$

The heat transfer rate in the condenser is calculated using the effectiveness-NTU method. The effectiveness (ξ) of a concentric heat exchanger is evaluated as follows Incropera [24]:

$$\xi_a = \frac{Q_{cond}}{\dot{C}_{min}(T_2 - T_{wi})} \tag{15}$$

$$\xi_b = \frac{1 - \exp[-\text{NTU}(1 - \dot{C}_{min}/\dot{C}_{max})]}{1 - \exp[-\text{NTU}(1 - \dot{C}_{min}/\dot{C}_{max})]\dot{C}_{min}/\dot{C}_{max}} \tag{16}$$

where $\dot{C}_{min}$ and $\dot{C}_{max}$ is the equal to $\dot{C}_r$ or $\dot{C}_w$, whichever is smaller and bigger, respectively. The refrigerant and water heat capacity rate are given by:

$$\dot{C}_w = \dot{m}_w C_w \tag{17}$$

$$\dot{C}_r = \dot{m}_r \overline{C}_r \tag{18}$$

In these equations, the mean specific heat of the refrigerant ($\overline{C}_r$) is evaluated by EQ. 19 and the Number of Transfer Units (NTU) by EQ. 20.

$$\overline{C}_r = \frac{i_2 - i_3}{T_2 - T_3} \tag{19}$$

$$\text{NTU} = \frac{UA}{\dot{m}_w C_w} \tag{20}$$

The UA value is determined by:

$$UA = \left(\frac{1}{\overline{h}_r \pi D_{ii} L_{cond}} + \frac{ln(D_{ii}/D_{io})}{2\pi k L_{cond}} + \frac{1}{\overline{h}_w \pi D_{oi} L_{cond}} \right)^{-1} \tag{21}$$

where the D_{ii} is the inner diameter of inner tube (4.76mm), D_{oi} is the outer diameter of inner tube (6.35mm), L_{cond} is condenser length (5,5m), the mean water HTC ($\overline{h}_w$) is calculated using the correlations described by [25] for flow in annular regions, and the mean refrigerant HTC ($\overline{h}_r$) is calculated assuming that the enthalpy varies linearly with length and using the correlation of Gnielinski [18] for h_r if $i \geq i_V$ or $i \leq i_L$ and the correlation of Shah [26] if $i_L < i < i_V$.

To consider the heat loss at the water tank and in the connecting tubes before and after the condenser, Kong et al. [5] propose a heat leakage coefficient of 95% given by:

$$\zeta = \frac{Q_t}{Q_{cond}} \tag{22}$$

2.4 Performance indicators

The coefficient of performance (COP) of DX-SAHP defined as follow [5, 19, 27]:

$$COP = \frac{\zeta \cdot \dot{Q}_{cond}}{\dot{W}} \tag{23}$$

In order to compare the accuracy of the model, the most used metrics are the Mean Absolute Deviation (MAD) and Mean Deviation (MD). For COP the MAD and MD are evaluated as showed in EQ. 24 and 25. The compressor outlet temperature (T_2) is calculated in similar way.

$$\text{MAD} = \frac{1}{n} \sum_{j=1}^{n} \left| \frac{COP_{calc} - COP_{exp}}{COP_{exp}} \right| \tag{24}$$

$$\text{MD} = \frac{1}{n} \sum_{j=1}^{n} \left(\frac{COP_{calc} - COP_{exp}}{COP_{exp}} \right) \tag{25}$$

2.5 Numerical procedure

In fact, the pressure of the refrigerant is not known and cannot be obtained from of the equations present so far. An algorithm for calculate this pressure was presented by Kong et al. [5], but in this study the author used a DX-SAHP immersed condenser and the mass of refrigerant is an input of the model. An algorithm explaining how these pressures are obtained is shown in Fig. 2 for a DX-SAHP with coaxial condenser. The secant method mentioned in Fig. 2 is described in detail by Chapra et al. [28]. The errors E_e and E_c, in percent, is given by:

$$E_e = \left| \frac{\dot{Q}_{re} - \dot{Q}_{col}}{\dot{Q}_{re}} \right| \cdot 100 \tag{26}$$

$$E_c = \left| \frac{\xi_a - \xi_b}{\xi_a} \right| \cdot 100 \tag{27}$$

To reduce the computational time the the final values for evaporating and condensation pressures is used as initial guess for the next simulation.

The output variables of the DX-SAHP model were calculated considering the uncertainties from the input variables. The measurements involved in this work are considered random and uncorrelated, and evaluated according to BIPM at al. [29].

3 Results

The model validation is performed comparing the experimental results using a TEV presented by [15] combined by the data available in Brazilian National Institute of Meteorology (INMET) web site. The comparison between measured and calculated COP and outlet compressor temperature is shown in the Tab. 1. The subcooling

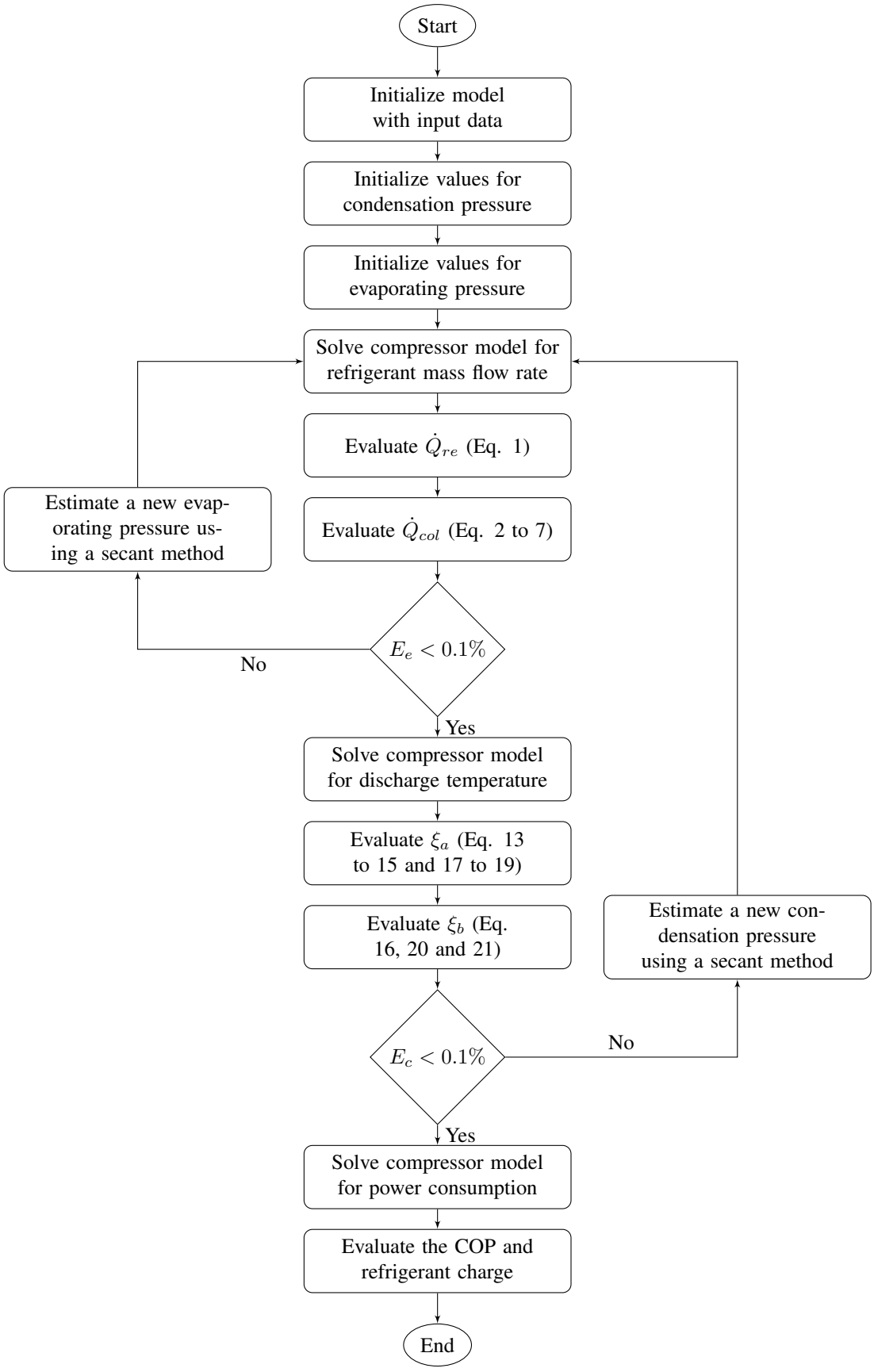

Figure 2. Model calculation algorithm.

was assumed fixed in 6.5^{o}C, which represents the average value in the experimental tests. In table 1, the uncertainty of the water inlet temperature (T_{wi}), water outlet temperature T_{wo} and ambient temperature (T_a) is $\pm 1^o$C, for dew point temperature (T_{dp}) is $\pm 2^o$C, for the superheating at exit of evaporator (ΔT_{sh}) is $\pm 1.4^o$C, for the atmospheric pressure $\pm$2kPa, for the solar radiation (I) is $\pm$5% and for wind speed (u_w) is $\pm$3%. The experimental results present good accuracy, 5.2% of uncertainty for COP and 1.4% for discharge temperature.

The MAD and MD of COP are respectively 4.2$\pm$4.8% and 2.9$\pm$5.2%. Considering the uncertainty range there is no mean difference of experimental COP and calculated COP. The MAD and MD of compressor outlet temperature are respectively 7.8$\pm$2.0% and 5.1$\pm$2.0%. The MAD and MD of compressor outlet temperature considering only the tests 6 to 10 are respectively 3.3$\pm$2.0% and -2.0$\pm$2.0%. Considering the uncertainty range and the experimental test with solar radiation, the most import for this work, there is no mean difference of experimental discharge temperature and calculated discharge temperature. For COP, the uncertainty of the model was four time lower than obtained experimentally. For discharge temperature, the uncertainty of the model was higher than that obtained experimentally.

Table 1. Results of experimental modeling validation

Test	Date	T_a	P_{atm}	T_{dp}	I	u_w	T_{wi}	T_{wo}	ΔT_{sh}	T_2		COP	
	dd/mm/yy	^{o}C	kPa	^{o}C	W/m^2	m/s	^{o}C	^{o}C	^{o}C	Exp.	Calc.	Exp.	Calc.
1	12/01/17	27.1	91.5	17.2	0	0	27.3	44.8	7.1	71.1$\pm$1.0	63.8$\pm$1.1	2.37$\pm$0.12	2.19$\pm$0.03
2	13/01/17	26.6	91.5	20.2	0	0	26.3	45.3	7.1	72.0$\pm$1.0	63.4$\pm$1.1	2.25$\pm$0.12	2.20$\pm$0.03
3	16/01/17	24.9	91.7	19.4	0	0	25.0	46.0	7.1	72.2$\pm$1.0	62.7$\pm$1.1	2.26$\pm$0.11	2.20$\pm$0.03
4	17/01/17	26.1	91.5	17.2	0	0	25.1	46.0	7.1	72.6$\pm$1.0	62.9$\pm$1.1	2.36$\pm$0.12	2.20$\pm$0.03
5	19/01/17	26.5	91.7	18.4	0	0	25.8	45.5	7.1	72.1$\pm$1.0	63.1$\pm$1.1	2.32$\pm$0.12	2.20$\pm$0.03
6	23/01/17	29.7	91.9	15.6	421	0.52	27.6	46.7	7.8	73.2$\pm$1.0	70.8$\pm$1.1	2.56$\pm$0.13	2.47$\pm$0.04
7	25/01/17	32.9	92.0	16.3	709	0.86	28.7	47.4	7.8	74.7$\pm$1.0	76.8$\pm$1.1	2.72$\pm$0.14	2.62$\pm$0.04
8	25/01/17	32.7	92.0	16.6	758	0.95	29.3	47.3	7.8	75.4$\pm$1.0	77.8$\pm$1.1	2.64$\pm$0.14	2.63$\pm$0.04
9	27/01/17	32.5	92.1	13.5	629	1.16	29.0	45.9	7.8	73.9$\pm$1.0	74.9$\pm$1.2	2.69$\pm$0.14	2.60$\pm$0.05
10	28/01/17	31.2	92.1	13.3	811	1.36	29.0	47.8	7.8	73.7$\pm$1.0	78.2$\pm$1.2	2.48$\pm$0.13	2.64$\pm$0.04

4 Conclusions

In this work a mathematical model of a R-134a DX-SAHP for producing domestic hot water is used to compare the performance between the simulation results and the experimental measurements. Compressor discharge temperature and thermal efficiency were compared. The mathematical model presented is this work is based in lumped model for the heat exchangers. The model was validated using 10 experimental testes performed in different environmental conditions.

The results show, considering the uncertainty range and the experimental test with solar radiation, there is no mean difference of experimental discharge temperature and calculated discharge temperature. For COP, the uncertainty of the model was four times lower than obtained experimentally. The MAD and MD of COP are respectively 4.2$\pm$4.8% and 2.9$\pm$5.2%. For the compressor outlet temperature considering only the tests 6 to 10 the MAD and MD are respectively 3.3$\pm$2.0% and -2.0$\pm$2.0%.

References

[1] Chua, K., Chou, S., & Yang, W., 2010. Advances in heat pump systems: A reveiw. *Applied Energy*, vol. 87, pp. S3611–S3624.

[2] Chaturvedi, S., Chen, D., & Kheireddine, A., 1998. Thermal performance of a variable capacity direct expansion solar-assisted heat pump. *Energy Conversion and management*, vol. 39, n. 3, pp. 181–191.

[3] Hawlader, M., Chou, S., & Ullah, M., 2001. The performance of a solar assisted heat pump water heating system. *Applied Thermal Engineering*, vol. 21, n. 10, pp. 1049 – 1065.

[4] Chyng, J., Lee, C., & Huang, B., 2003. Performance analysis of a solar-assisted heat pump water heater. *Solar Energy*, vol. 74, n. 1, pp. 33 – 44.

[5] Kong, X., Zhang, D., Li, Y., & Yang, Q., 2011. Thermal performance analysis of a direct-expansion solar-assisted heat pump water heater. *Energy*, vol. 36, n. 12, pp. 6830–6838.

[6] Moreno-Rodríguez, A., González-Gil, A., Izquierdo, M., & Garcia-Hernando, N., 2012. Theoretical model and experimental validation of a direct-expansion solar assisted heat pump for domestic hot water applications. *Energy*, vol. 45, n. 1, pp. 704–715.
[7] Mohamed, E., Riffat, S., & Omer, S., 2017. Low-temperature solar-plate-assisted heat pump: A developed design for domestic applications in cold climate. *International Journal of Refrigeration*, vol. 81, pp. 134 – 150.
[8] Duarte, W. M., Paulino, T. F., Pabon, J. J., Sawalha, S., & Machado, L., 2019. Refrigerants selection for a direct expansion solar assisted heat pump for domestic hot water. *Solar Energy*, vol. 184, pp. 527 – 538.
[9] Chata, F. G., Chaturvedi, S., & Almogbel, A., 2005. Analysis of a direct expansion solar assisted heat pump using different refrigerants. *Energy Conversion and Management*, vol. 46, n. 15, pp. 2614–2624.
[10] Kara, O., Ulgen, K., & Hepbasli, A., 2008. Exergetic assessment of direct-expansion solar-assisted heat pump systems: review and modeling. *Renewable and Sustainable Energy Reviews*, vol. 12, n. 5, pp. 1383–1401.
[11] Omojaro, P. & Breitkopf, C., 2013. Direct expansion solar assisted heat pumps: A review of applications and recent research. *Renewable and Sustainable Energy Reviews*, vol. 22, pp. 33 – 45.
[12] Mohanraj, M., Belyayev, Y., Jayaraj, S., & Kaltayev, A., 2018a. Research and developments on solar assisted compression heat pump systems – A comprehensive review (Part A: Modeling and modifications). *Renewable and Sustainable Energy Reviews*, vol. 83, pp. 90 – 123.
[13] Mohanraj, M., Belyayev, Y., Jayaraj, S., & Kaltayev, A., 2018b. Research and developments on solar assisted compression heat pump systems – A comprehensive review (Part-B: Applications). *Renewable and Sustainable Energy Reviews*, vol. 83, pp. 124 – 155.
[14] Rabelo, S. N., Paulino, T. F., Machado, L., & Duarte, W. M., 2019. Economic analysis and design optimization of a direct expansion solar assisted heat pump. *Solar Energy*, vol. 188, pp. 164 – 174.
[15] Diniz, H. A. G., 2017. Estudo comparativo da eficiência energética de uma bomba de calor assistida por energia solar operando com condensadores por imersão e coaxial. Master's thesis, UFMG, Belo Horizonte, MG, Brazil.
[16] Duffie, J. A. & Beckman, W. A., 2013. *Solar engineering of thermal processes*. John Wiley & Sons.
[17] Shah, M. M., 2017. Unified correlation for heat transfer during boiling in plain mini/micro and conventional channels. *International Journal of Refrigeration*, vol. 74, pp. 604–624.
[18] Gnielinski, V., 1976. New equations for heat and mass transfer in turbulent pipe and channel flow. *Int. Chem. Eng.*, vol. 16, n. 2, pp. 359–368.
[19] Kong, X., Li, Y., Lin, L., & Yang, Y., 2017. Modeling evaluation of a direct-expansion solar-assisted heat pump water heater using R410A. *International Journal of Refrigeration*, vol. 76, pp. 136–146.
[20] Gliah, O., Kruczek, B., Etemad, S. G., & Thibault, J., 2011. The effective sky temperature: an enigmatic concept. *Heat and mass transfer*, vol. 47, n. 9, pp. 1171–1180.
[21] Berdahl, P. & Fromberg, R., 1982. The thermal radiance of clear skies. *Solar Energy*, vol. 29, n. 4, pp. 299 – 314.
[22] Neils, G. & Klein, S., 2009. *Heat Transfer*. Cambridge university press.
[23] Minetto, S., 2011. Theoretical and experimental analysis of a CO_2 heat pump for domestic hot water. *International journal of refrigeration*, vol. 34, n. 3, pp. 742–751.
[24] Incropera, F. P., Lavine, A. S., Bergman, T. L., & DeWitt, D. P., 2007. *Fundamentos da Transferência do Calor e massa*. Editora LTC, 6 edition.
[25] Duarte, W. M., 2018. *Numeric model of a direct expansion solar assisted heat pump water heater operating with low GWP refrigerants (R1234yf, R290, R600a and R744) for replacement of R134a*. PhD thesis, UFMG.
[26] Shah, M. M., 2016. Comprehensive correlations for heat transfer during condensation in conventional and mini/micro channels in all orientations. *International journal of refrigeration*, vol. 67, pp. 22–41.
[27] Kuang, Y., Sumathy, K., & Wang, R., 2003. Study on a direct-expansion solar-assisted heat pump water heating system. *International Journal of Energy Research*, vol. 27, n. 5, pp. 531–548.
[28] Chapra, S. C. & Canale, R. P., 2008. *Métodos numéricos para engenharia*. McGraw-Hill.
[29] BIPM, I., IFCC, I., IUPAC, I., & ISO, O., 2008. *Evaluation of measurement data—Guide for the expression of uncertainty in measurement. JCGM 100: 2008*.